HSPI The Open Access Publisher

IJCV INTERNATIONAL JOURNAL OF CLINICAL VIROLOGY
ISSN 2692-4994

Research Article

Coronaviruses have reached at Pre-elimination Stage with Nine Amino Acid Spike Deletions and Forty-nine Nucleotide 3'-UTR Deletions

Asit Kumar Chakraborty*

Department of Biochemistry and Biotechnology, Vidyasagar University, West Bengal, India

Abstract

Background: Human 30kb coronaviruses entered through the ACE-2 receptors causing fibrosis of the lungs and causing six million deaths worldwide. Here, we have investigated the mutations, deletions and insertions of the recent JN.1 omicron coronaviruses to demonstrate that coronaviruses have reached the pre-elimination stage.

Methods: We multi-aligned the genomes of recent JN.1 variants using NCBI Virus Portal and CLUSTAL-Omega. The spike proteins are multi-aligned using MultAlin software and CLUSTAL-Omega.

Results: The ^{17}MPLF spike insertion was confirmed to compensate ^{24}LPP, ^{31}S, ^{69}HV, ^{145}Y, ^{211}N and ^{483}V deletions. The 49nt deletions in the 3'-UTR were found in 4997 JN.1 sequences although 26nt deletion was initiated previously in JN.1 as well as BA.5, BF.7, BQ.1 and XBB.1.5 omicron viruses. We first compare 3-D structures of spike proteins with or without ^{17}MPLF four amino acids insertion and nine amino acids deletions using SWISS MODELLING. The JN.1 viruses caused a more stable trimeric spike involving Thr342, Lys436, Lys440, His441, Ser442, Gly443, Tyr445, Lys479, Ser489, Tyr490, Arg493, Pro494, Thr495, and Gln501 amino acids to interact with ACE-2 receptors. The FLiRT spike mutations were found in most KP.2 variants and other changes occurred at the NH_2 terminus.

Conclusion: We claimed that pre-death changes were initiated in JN.1 COVID-19 lineages and computer simulation showed that the Howard spike with ^{17}MPLF spike insertion appeared more stable than the Oppentrons-spike without ^{17}MPLF insertion. Surely, conflicts of COVID-19 spike sequences must be resolved.

More Information

***Address for correspondence:**
Asit Kumar Chakraborty, Department of Biochemistry and Biotechnology, Vidyasagar University, West Bengal, India,
Email: chakraakc@gmail.com

Submitted: September 06, 2024
Approved: September 16, 2024
Published: September 17, 2024

How to cite this article: Chakraborty AK. Coronaviruses have reached at Pre-elimination Stage with Nine Amino Acid Spike Deletions and Forty-nine Nucleotide 3'-UTR Deletions. Int J Clin Virol. 2024; 8(2): 031-044. Available from: https://dx.doi.org/10.29328/journal.ijcv.1001060

Keywords: COVID-19 pre-elimination stage; Spike ^{17}MPLF insertion mutants; ^{31}S spike deletion; KP.2 subvariant; 49nt deletion in 3'-UTR; Fraudulent data deposition

Introduction

About seven million people died due to coronavirus infection worldwide between 2019 and 2024 [1-5]. Vaccination and autoimmunity greatly controlled the epidemic but omicron coronavirus mild infection is still happening today [6-9]. Nevertheless, patients with co-morbidity and old age still are dying due to omicron infections. The United States and the United Kingdom are continuing their WGS sequence analysis from samples isolated from newly coronavirus-infected people. The great VOC of coronavirus classification were Alpha with N501Y spike mutation, Delta with D614G, L452R, T478K, P681R and A222V spike mutations including P1, P2, Beta and Gamma and a few omicron variants that were affected greatly between 2020-2023 [10-14]. While Omicron BA.1 followed by BA.2, BA.3, BA.4 and BA.5 affected with great specificity worldwide between 2023-2024 with lower severity [15]. The major point mutations in the spike protein of different omicron coronaviruses were demonstrated in Table 1 and more mutations were depicted in the recent JN.1 variant. The major deletions and insertions in the spike protein of different coronavirus variants are shown in Table 2.

The BA.4 and BA.5 variants' mutations are very similar (protein id. URO63244). The BF.7 is very similar to BA.5 but BF.7 specific spike mutations were reported as T76I (I71) and R346T (T341) (protein id. UZM66933). The XBB was generated through recombination between BA.2.10.1 and BA.2.75 with many mutations as in BA.2 and V83A, Y145 del, H146Q, Q183E, V213E, G252V, G339H, R346T, L368I, V445P, G446S, N460K, F486S and F490S. The XBB.1.5 variant spike mutations were reported as L455F, F456L, N460K, S486P and F490S. Otherwise, if a higher transmissible less pathogenic omicron virus with 30 mutations in the spike was not generated, then notorious Delta COVID-19 might claim more few million deaths. Thus, in my opinion, Omicron infection was a blessing for us but Covisheild, Covaxin and related mRNA vaccines were partially effective for omicron infection. Thus, we found repeated coronavirus infections after vaccination worldwide between 2022 and 2024 [16]. COVID-19 preferably infects human lung cells and enters through the interacting trimeric spike protein of coronavirus and human ACE-2 receptor. Spike protein is 1273aa in Wuhan (2019) but greatly varied in different lineages [17]. In the Alpha lineage spike changed to 1270aa due to deletions of ^{69}HV and ^{145}Y positions whereas in the Delta variant spike changed to 1271AA due to ^{156}FR deletion only (2021-2022). Spike

protein of omicron BA.1 variant is 1270AA due to ^{69}HV, ^{143}VYY and ^{212}L deletions as well as ^{215}EPE three amino acid insertion. The Spike protein of omicron BA.4 and BA.5 coronaviruses is 1268AA due to deletions of ^{24}LPP and 69HV. Spike protein of omicron BA.2 has 1270AA due to ^{24}LPP deletion only (2022-2023). The ^{69}HV spike deletion was first found in B.1.1.7 but also acquired in omicron BA.1, BA.4 and BA.5 variants but not in the omicron BA.2 variant until BA.2.86.1 or JN.1 appeared at the end of the year 2023 [18-20]. Among the other structural proteins N-protein (419aa) binds to leader RNA of replicating coronavirus and also regulates host-pathogen interactions. Three AAs deletions (^{31}ERS) were found in N-protein (416aa) of all omicron coronaviruses. Three amino acid deletions (^{3675}SGF) were found in ORF1ab protein (nsp6 protein region) of Alpha and Omicron BA.2 and BA.5 including BQ.1, BF.7, XBB.1 and JN.1 (ORF1ab=7093aa) but at the same region ^{3674}LSG deletion, as well as extra 2083S deletion, were found in omicron BA.1 coronavirus (ORF1ab=7092aa). Interestingly, no ORF1ab deletions in the notorious Delta variant (ORF1ab=7096aa). Whereas, a three amino acids ^{141}KSF deletion in the nsp1 protein was found in omicron BA.4 variant only (ORF1ab=7090 AAs). The P4715L ORF1ab mutation at RdRP (P323L) was found in all variants since March 2020 similar to the D614G mutation and suggested as a modulator of transmission [21]. As N501Y and D614G both mutations appeared in omicron BA.1, BA.2, BA.4, BA.5, BQ.1, XBB.1 and JN.1 viruses and gained more spread than alpha, beta or delta variants but gave mild pathogenicity due to 25 more mutations in the spike and 26nt 3'-UTR deletion [20]. The L452Q mutation facilitated immune escape in BA.2.12 and BA.2.75 sub-lineages carrying additional R346T, F486S and D1199N mutations and rearrangement to produce XBB variant. Delta variant had L452R immune-escape mutation which was also gained by omicron BA.1 as well as BA.4 and BA.5 variants. The BA.4 and BA.5 variants also gained important F486V mutation to produce immune escape similar to the L452R mutation. We also characterized the ORF7a deletion in many coronaviruses lineages including B.1.1.7 and BQ.1 whereas BQ.1 specific K444T and N460K mutations were reported [22]. Similarly, the different termination codon mutations were detected to abolish the expression of small ORF8 protein that targets cellular immunogenic proteins [23,24]. The new mutations cluster was reported in BA.2.86 that was later named as JN.1. The JN.1 important spike mutations were reported as ^{17}MPLF ins, ^{24}LPP del, ^{69}HV del, ^{145}Y del, ^{211}N del, ^{384}V del, ^{1332}V, D339H, R403K, V445H, G446S, N450D, L452W, N481K, 483V del, E484K, F486P, N501Y and D614G. Recently we communicated the expansion of omicron JN.1 lineages with ^{17}MPLF spike insertion compensating ^{24}LPP, (31S) ^{69}HV, ^{145}Y, ^{211}N and ^{483}V deletions (NC_045512.2 positions) with decrease in HV.1, XBB.1 and BN.1, EG.1, and FL.1 lineages [20]. We have also shown further expansion of ^{17}MPLF insertion mutant in different new omicron lineages including JN.1.1-JN.1.25, KP.1, KQ.1, KR.1, KP.2, KP.1.1, XDD, XDP, XDQ, XDQ.1, LA.1, LB.1, KS.1.1, LF.1.1 and LW.1 subvariants [25]. The article further showed the JN.1 development with 49nt deletion in the 3'-UTR (~0.1% of 26nt 3'-UTR deletion) and other insertions and deletions.

Methods

Coronavirus sequences were obtained from the NCBI Virus Database (NIH, USA) between June-August, 2024. The virus collection time and RNA sequence deposited a time gap of as low as 15 days and coronavirus spread in the USA could be known with time. The spike protein sequence with AAs 1268 was due to nine deletions and four insertions of amino acids in ^{17}MPLF spike insertion mutants. The KP.2, KP.3, LB.1, LP.1 and KS.1 new subvariants were analysed separately if necessary. We collected various subvariants based on multi-alignment of spike proteins and virus sequences using CLUSTAL Omega software (www.ebi.ac.uk/jdipacher/msa/clustalo) or NCBI Virus Portal. Multiple copies of single subvariant populations were analysed using the NCBI Virus Portal [26,27]. Analysis of mutant proteins was done by BLASTP search with mutant-peptide (www.ncbi.nlm.nih.gov/blastp) [28,29]. The hairpin RNA structure was found by OligoAnalyzer 3.2 software. Homology modelling of protein structures and complexes was performed using SWISS-MODELLING [30-33]. The dates were given here as day/month/year. The original nomenclature of new variants has been documented as follows: JN.1 (BA.2.86.1.1), KP.2 (JN.1.11.1.2), LA.1 (JN.1.16.2.1), KS.1 (JN.1.13.1.1), KQ.1 (JN.1.4.3.1) and LB.1 (JN.1.9.2.1).

Results and discussions

Human coronavirus is a 30kb positive sense ss-RNA virus which transcribes two large polyproteins as well as four structural proteins (Figure 1). The WGS has been performed since 2019 till now as COVID-19 claimed six million deaths [9]. We are tracking the NCBI SARS-CoV-2 database to monitor the point mutations, deletions and insertions of different coronavirus variants (Figure 2). In Figure 3, we demonstrated the ^{17}MPLF spike insertion as well as ^{24}LPP deletion and ongoing ^{31}S deletion of JN.1 coronaviruses as deposited by Howard D, et al. on 23.7.2024. Similarly, in Figure 4 we demonstrated the JN.1 sequences deposited by other workers worldwide. The Figure 4A demonstrated the ^{17}MPLF spike protein insertion in Virginia State deposited by Finkelstein, et al, Figure 4B by Tsaknaridis, et al. from Oregon State, Figure 4C by Russian scientist Krylova, et al. deposited on 28.7.2024, Figure 4D by Heibeck N, et al. from Los Angles with +^{17}MPLF insertion, Figure 4E by Acevedo-Marquez L, et al. from Puerto Rico islands, Figure 4F from New York coronaviruses deposited by Moscovitz S, et al. on 5.8.2024 and Figure 4G deposited on 15.8.2024 by Rothstein AP, et al. of Washington State. Thus, ^{17}MPLF spike insertion to compensate for nine amino acid deletions was found by most workers [20].

We discussed earlier that Oppentrons P continuously deposited JN.1 sequences without ^{17}MPLF spike insertion. In Figure 5A, we showed the multi-alignment of JN-viruses deposited by Oppentrons P on 26.7.2024 and Figure 5B showed the more JN.1 lineages namely, JN.1.11.1, JN.1.16

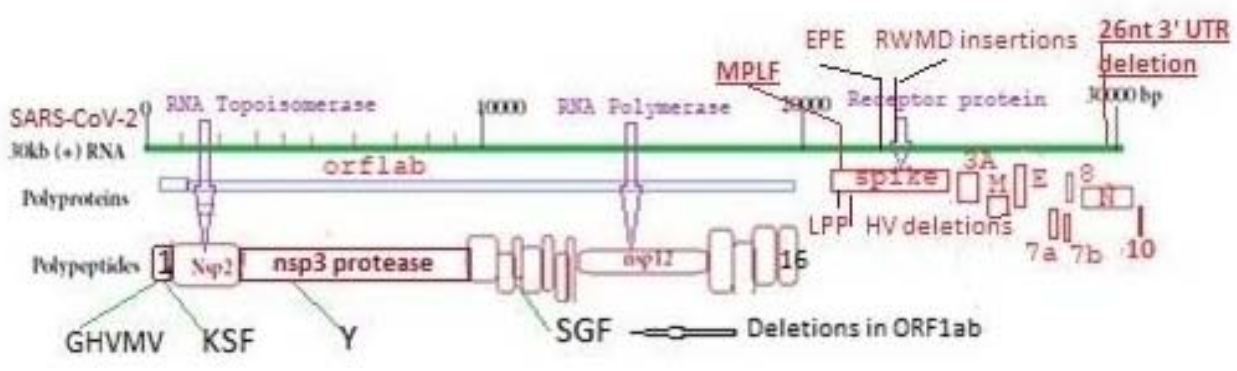

Figure 1: Structure of 30kb single-stranded human corona RNA virus.

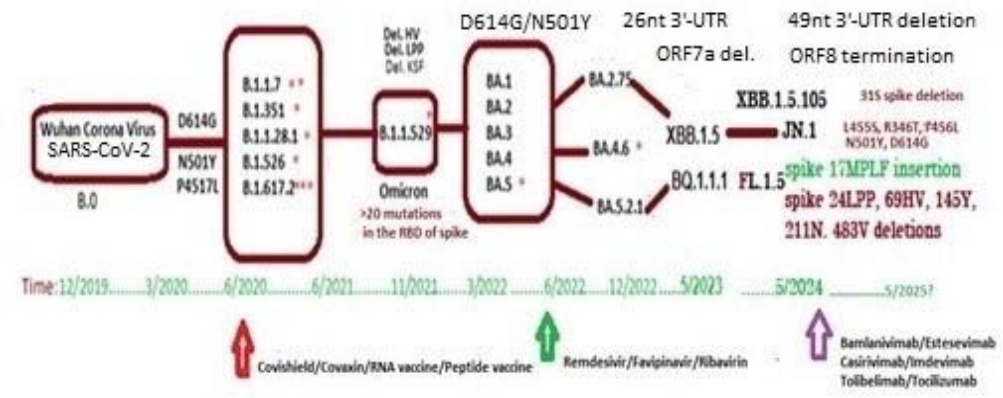

Figure 2: Genetic changes with time with the generation of different VOC of coronaviruses.

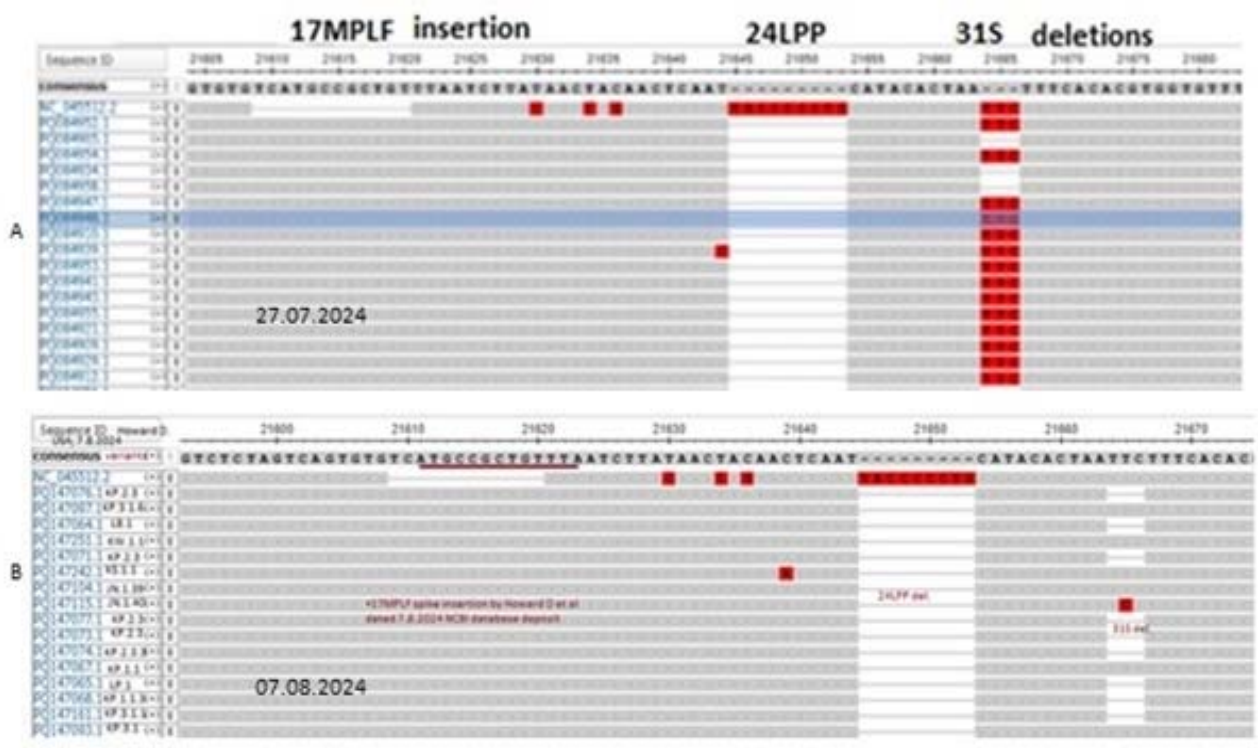

Figure 3: Multi-alignment of JN.1 coronavirus spike NH_2 terminus deposited by Howard D et al on 26.7.2024 and 7.8.2024 showing ^{17}MPLF spike insertion.

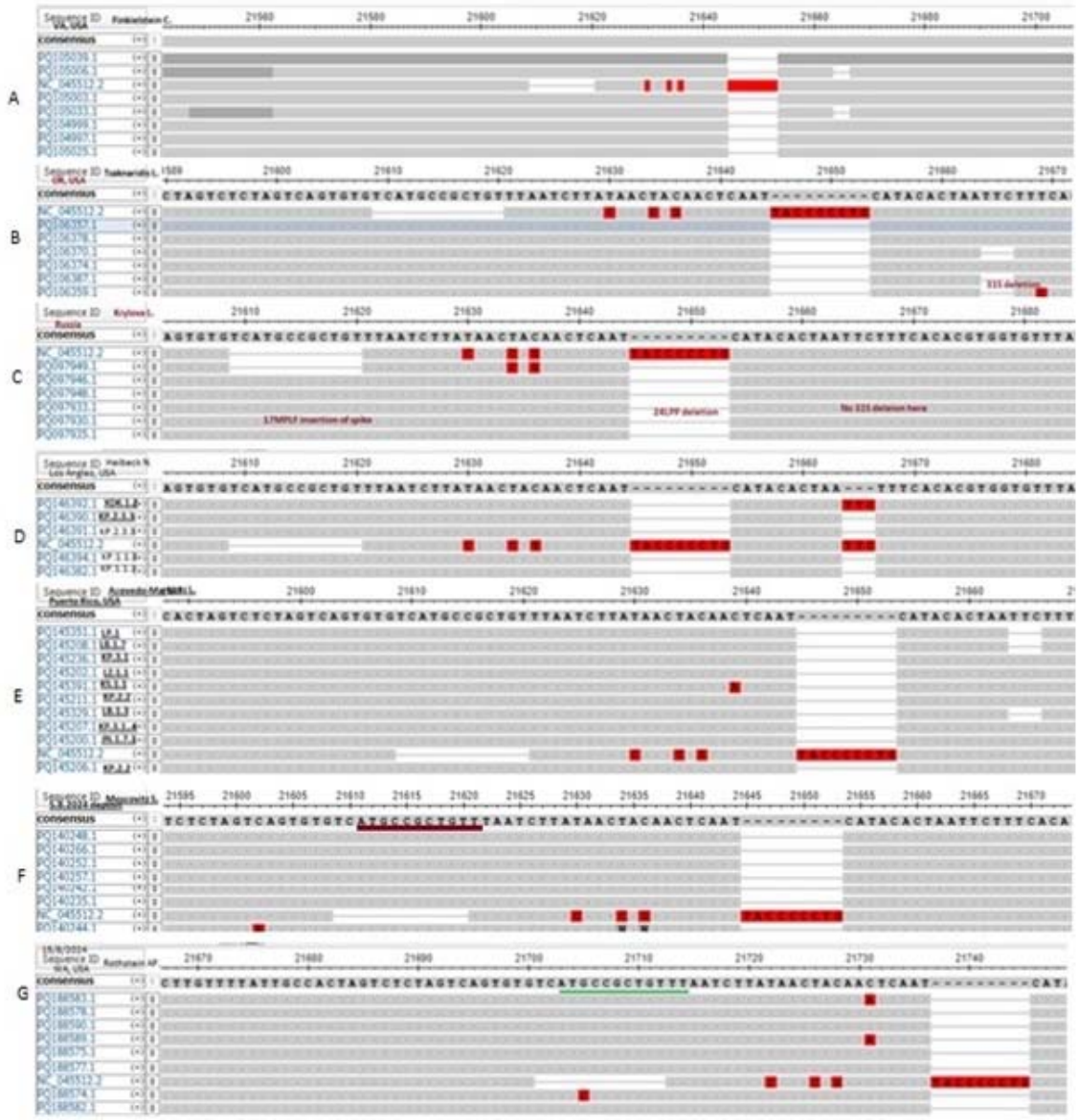

Figure 4: Demonstration of [17]MPLF spike protein insertion by different workers that compensated nine AAs deletions. (A) in Verginia State JN.1 coronavirus deposited by Finkelstein, et al. (B) in Oregon State sequenced by Tsaknaridis, et al. (C) in Russia by Krylova NV, et al, (D) in Los Angles deposited by Heibeck N, et al. (E). In Puerto Rico islands deposited by Acevedo-Marquez L, et al. (F) in New York deposited by Moscovitz S, et al. and (G) in Washington State deposited by Rothstein AP, et al.

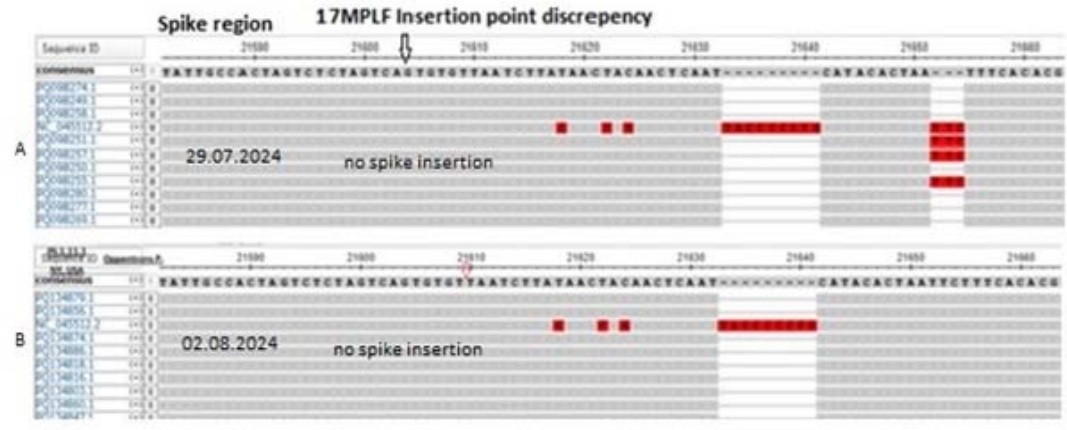

Figure 5: The multi-alignment of SARS-CoV-2 genomes by Oppentrons P to demonstrate no [17]MPLF spike insertion contrary to Figure 3 and Figure 4. The viruses were isolated from New York City on 29.07.2024 (A) and 2.8.2024 (B)

and KP.2 omicron viruses deposited on 2.8.2024 without ^{17}MPLF spike insertion. Similarly, Atkins (Louisiana, USA) also deposited many JN.1 sequences with no ^{17}MPLF spike insertion but respective deletions (^{24}LPP, ^{69}HV, ^{145}Y, ^{211}N etc) were there (data not shown). Sadly, we found no 26nt deletion in the 3'-UTR (Figure 6). We thought that proper sequencing was not done and fabricated data was deposited! Previously, we demonstrated that Sadri N, et al. also deposited data without ^{17}MPLF spike insertion (Research Square, 15th July 2024)

The ^{17}MPLF spike insertion seems to be a big controversy. So, we wanted to check the FLiRT mutation status of KP.2 variants from different workers with or without ^{17}MPLF spike insertion. In Figure, we showed the multi-alignment of spike proteins to demonstrate spike ^{17}MPLF insertion as well as ^{24}LPP, ^{31}S and ^{69}HV deletions. Surely, Oppentrons, Reev and Atkins data indicated no ^{17}MPLF insertion but other deletions were confirmed. But Howard, Gariques, Bondar, Estes, Linares, Price and Lauring declared the ^{17}MPLF spike insertion in KP.2 variants from different States (Figure 7A). Similarly, FLiRT mutations in KP.2 variants were found in all cases whether the spike ^{17}MPLF insertion was there or not (Figure 7B). But Matzinger data of the KP.2 variant showed the absence of R346L and F456L mutations. We also cross-checked the ^{145}Y and ^{211}N deletions which were also the hallmarks of JN.1 lineages and FLiRT variants.

Next, we compared the deletion points of both 26nt and 49nt 3'-UTR deleted genomes as demonstrated in Figure 8. The multi-alignment of the spike of 49nt 3'-UTR deleted coronavirus helps to understand that such deletion was initiated in the Alpha variant (AN: MZ188143, OQ521205) as well as in Delta (AN: OL738459) during 2021 as well as in Omicron BA.1 (AN: OM539704). Such viruses were predominant in the US (AN: PQ075568), UK (AN: OZ121939) as well as in Africa (AN: OQ521205. We also showed the difference in hairpin stem and loop structures among deleted 3'-UTR that were the binding sites of N-protein and perhaps human cellular regulatory factors (Figure 9) [34]. The human miRNAs and transfer RNA-derived RNAs (tDRs) were shown to target SARS-CoV-2 3'-UTR and might be involved in the regulation of gene expression and are associated with cancer and viral infections [35]. The 3'-UTR of coronavirus was shown to interact with piRNAs [36]. The SARS-CoV-2-encoded small RNAs are able to repress the host expression of SERINC5 to facilitate viral replication [37-39]. Such analysis helped us to conclude that coronavirus had reached a pre-elimination stage. The ds-RNA genome formation, virus assembly and transcription of structural proteins were inhibited due to the absence of intact 3'-UTR with the reduced viral titre [40]. So, the power of coronavirus to cause the fibrosis of lungs might not be possible for those with COVID-19. We also showed the nine amino acids deletion in the NH_2 terminus of spike protein that interacted in trimeric forms to ACE-2 receptor of lung cells as well other cells in the respiratory tract (Figure 1). We also postulated that Nsp2 and Nsp13 proteins were packaged into ribosomes due to their similarities with ribosomal proteins (L6, L9, L22) and also methylated the ribosomal RNAs inhibiting protein synthesis as well as ATP synthesis [41].

Truly, 26nt deletion in the 3'-UTR was well documented in omicron coronaviruses [42]. Here, we also showed the 49nt deletion in the 3'-UTR of thousands of sequences deposited in the NCBI database. But Atkins data (accession numbers: PQ100714-PQ100886) showed no deletions at the 3'-UTR boundary and we felt some problems in the sequencing (Figure 6). The viruses were collected in July 2024 from the Louisiana State of USA. The Oppentrons collected the coronaviruses from patients in the New York State. So, both

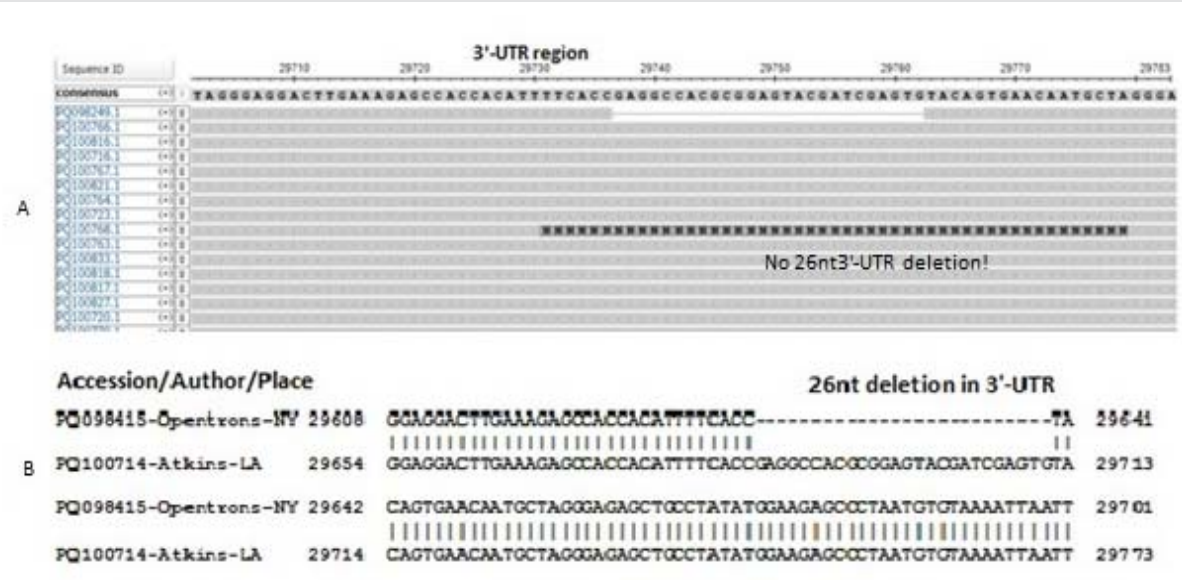

Figure 6: Multi-alignment of JN.1 coronavirus genome without 26nt 3'-UTR deletion deposited by Atkins on 29.07.2024 (Louisiana, USA) (A). (B) We BLAST-2 aligned two sequences (one with 26nt 3'-UTR deletion and one with no 26nt 3'-UTR deletion by Atkins). We argued that Howard D et al (figure-3) did correct sequencing and data deposition but Oppentrons and Atkins sequence data had many errors.

Figure 7: Multi-alignment of spike proteins of KP.2 variants isolated between May-July, 2024 to demonstrate FLiRT mutations. (A) [17]MPLF insertion region, (B) R346T mutation region and (C) L455S and F456L mutation region.

States are located in the East but far distance between the two States. Howard D, et al. reported the data from New York State demonstrating [17]MPLF insertion in the spike protein (see, accession numbers: OR642994, PP994450). We collected hundreds of sequences from New York and all had [17]MPLF spike insertion authenticating the data of Howard D, et al. We claimed that pre-death initiation in coronaviruses and support of such an idea we demonstrated the 49nt 3'-UTR deletion in our two searches during August 2024. For that, we have always checked the 3'-UTR area in our multi-alignments if 26nt or 49nt deletion or such area was not sequenced at all to avoid the controversy. For example, Price A, et al. did not sequenced the 3'-UTR regions (see, accession numbers: PQ167127-PQ167141; deposit date 16.8.2024). The 26nt 3'-UTR deletion was abundant in many omicron variants but the recent 49nt 3'-UTR deletion was very important in destabilizing the virus assembly. BLASTN search with 49nt deletion boundary (5'-GAAAGAGCCACCACATT/GGGAGAGCTGCCTATATG-3') detected thousands of such coronavirus genomes (accession numbers: PQ302876, PQ302645, PQ145235, PQ084932, PQ075568, PQ075518, PQ065717, PQ065673, OZ125311, OZ121939, OZ121689, OZ050410, OZ050038, OZ049909, OZ181360 and OP563917) (Figure 10). Figure 10a (accession no. PQ134886) and 10b (accession no. PQ124835) demonstrated that 49nt 3'-UTR deletion has been initiated and continuing today (see, red arrow). Recently, the 16.8.2024 data by Oppentrons again claimed no [17]MPLF spike insertion but we got a 49nt deletion in the 3'-UTR (see, accession number: PQ197438). We proved that data deposited by scientists varied and we should discuss the differences as we could not understand the fabricated data as the changes in the genetic structure of coronaviruses were very important to note (Research Square, 22 January 2024).

Figure 8: Multi-alignment comparison of the 26nt and 49nt deleted 3'-UTR of COVID-19 genomes. The 26nt deletion = 5'-^{29747}GTACGATCGAGTGTACAGTGAACAAT-3' and the 49nt deletion = 5'-^{29728}TTC ACC TAC AGT GAA CAA TGT ACG ATC GAG TGT ACA GTG AAC AAT GTT A-3'.

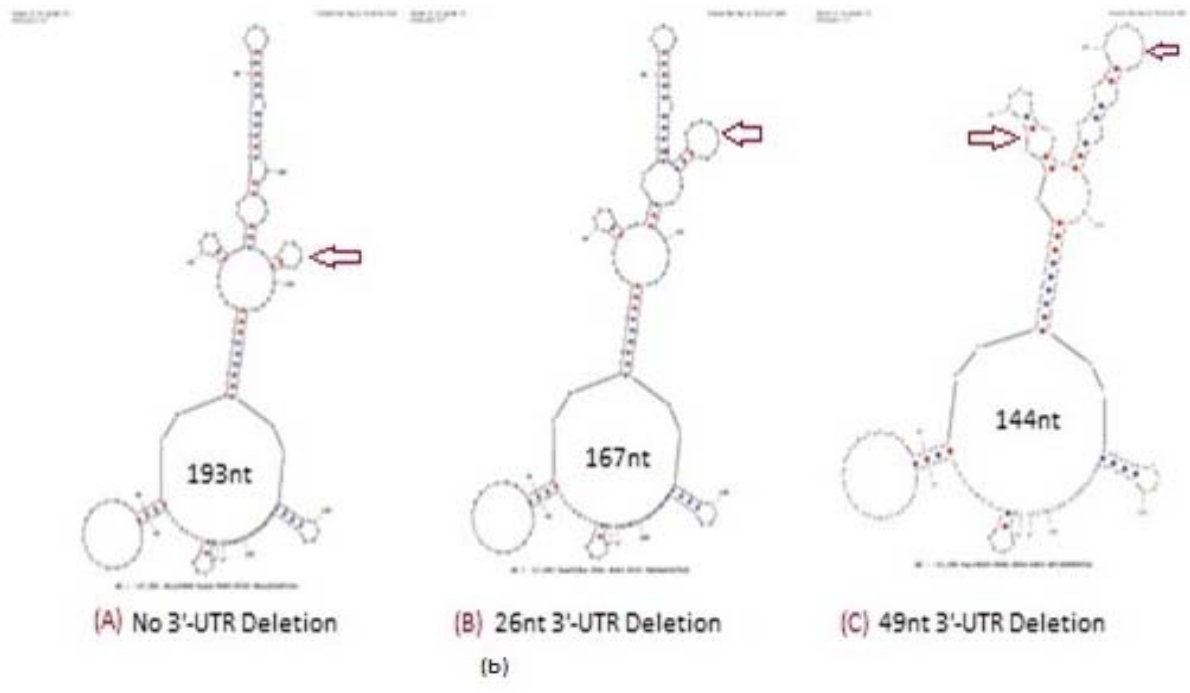

Figure 9: Hairpin structures of Coronavirus 3'-UTR (A), 26nt deleted 3'-UTR (B) and 49nt deleted 3'-UTR ©. Profound stem and loop structural changes were located by Oligo Analyzer 3.2 software (red arrows). Such sequence organization was the site for piRNA. Truly, two SARS-CoV-2 sequences, 29,792–29819 (hsa_piRNA_23,430) and 29,757–29784 (hsa_pRNA_25,334) reported as piRNA homology (Hernandez-Huerta et al. 2023; Pérez-Campos, et al. 2023).

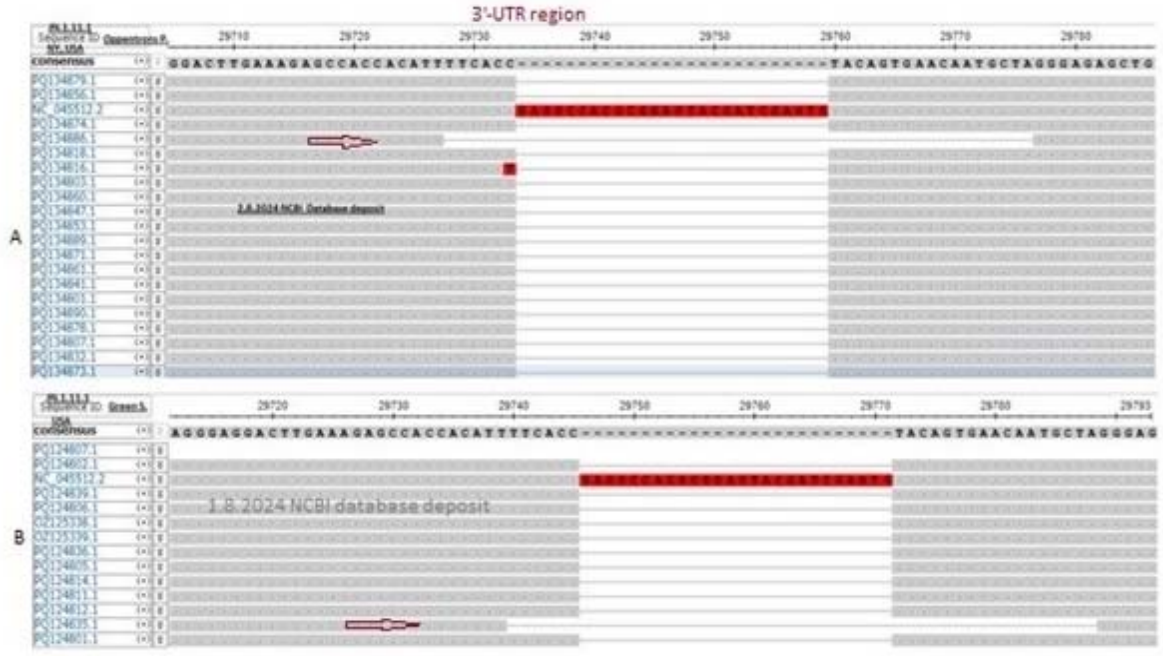

Figure 10: The demonstration of the spread of 49nt 3'-UTR deletion as obtained during multi-alignment in the background of 26nt 3'-UTR deletion. (A) Demonstrated the data by Oppentrons P on 2.8.2024 and (B) demonstrated the data by Green S, et al. on 1.8.2024 and the coronaviruses were JN.1.11.1 subvariants in both cases. Part of the alignments were shown and the red arrow indicated the 49nt 3'-UTR deletion.

We further checked the 3-D structures of a spike of Wuhan, Oppentrons-JN.1 and Howard-JN.1 coronaviruses using SWISS-Modelling Software (Figure 11). The accumulation of dominant mutations in JN.1 viruses caused a more stable trimeric spike involving Thr342, Lys436, Lys440, His441, Ser442, Gly443, Tyr445, Lys479, Ser489, Tyr490, Arg493, Pro494, Thr495, and Gln501 amino acids to interact with ACE-2 receptors (Figure 11A). The quality parameters of such modelling are given in Table 3 [43]. Here, we saw a higher QMQE value (0.69 *vs.* 0.68 in Table 3A; 0.68 *vs.* 0.67 in Table 3B) for Howard-spike than Oppentrons-spike [44]. We found higher (0.99 *vs.* 0.98 in Table 3A; 0.97 *vs.* 0.95 in Table 3B) spikes with four amino acid insertions to compensate for eight amino acid deletions for omicron JN.1 variant coronaviruses. The bad bonds were higher for the Oppentrons-spike in the case of Model-2 and Model-3. Thus, we concluded that $+^{17}$MPLF insertion mutants were favourable and formed better 3-D structures to make good interaction with the ACE-2 receptor of lung cells as well as respiratory cells of the nose and mouth cavity. We also found a higher Clash score with the spike of $+^{17}$MPLF insertion mutants (1.11 *vs.* 0.95 in Table 1A; 0.90 *vs.* 0.63 in Table 3B). Thus, in $+^{17}$MPLF spike more steric hindrance suggesting insertion and deletion were not allowed at any point of a spike of SARS-CoV-2. Thus, we hardly found any insertion or deletion in the RBD of the spike (315-525aa). However, neither we found the insertion and deletion in the C-terminus and only deletions and insertion in the spike were allowed between NH_2 terminus 1-250 amino acids. MolProbity data predicted a better Spike-ACE2 for $+^{17}$MPLF JN.1 COVID-19 variants [45].

We showed the 3-D structures of Howard-spike (protein id. XDF23570) with $+^{17}$MPLF insertion (PQ040957) as well as Oppentrons-spike (XBS50626) with no such four amino acids insertion (PP916085) although nine amino acids deletion were happened in recent JN.1 variants of COVID-19 (Figure 11). Thus, our interpretation that COVID-19 had entered a pre-elimination stage might not be a valuable comment. We found more compact 3-D spike structures in modelling with spikes of JN.1 coronavirus [46]. Similarly, nine amino acids deletions in spike ligand were not a favourable consequence, neither, 49nt deletion in the 3'-UTR of thousand coronavirus genomes was not a favourable genome stability of any virus and most omicron coronaviruses had at least 26nt 3'-UTR deletion. We also predicted an altered 3-D structure in the 3'-UTR of the RNA genome that interacted with many proteins for coronavirus assembly and transcription [40]. The ORF8 termination codon mutations and ORF7a/b deletions were also described to state the art of genome instability in coronaviruses [22,23]. We have seen that with the 8gtp.1.B template (BA.5 variant spike) both spikes formed only monomer 3-D structures while using the 8xu.1.A template (XBB.1.5 variant), trimer structures were produced. Similarly, with 8wly.1.B template (Bat spike origin) Oppentrons-spike did not form a compact structure and subunit-3 protruded upside (open complex) and did not form a symmetrical 3-D structure at all (data not shown). Similarly, why the 8gtp.1.B template and Oppentrons-spike did not make a favourable oligomeric 3-D structure with 96.28% similarity was not clear. We also checked the 3-D structure of the Wuhan spike with a QMQE score of 0.68 and a QSQE score of 0.98 but we saw less possible 3-D compactness in three subunits of the spike (data not shown). Such data reflected a

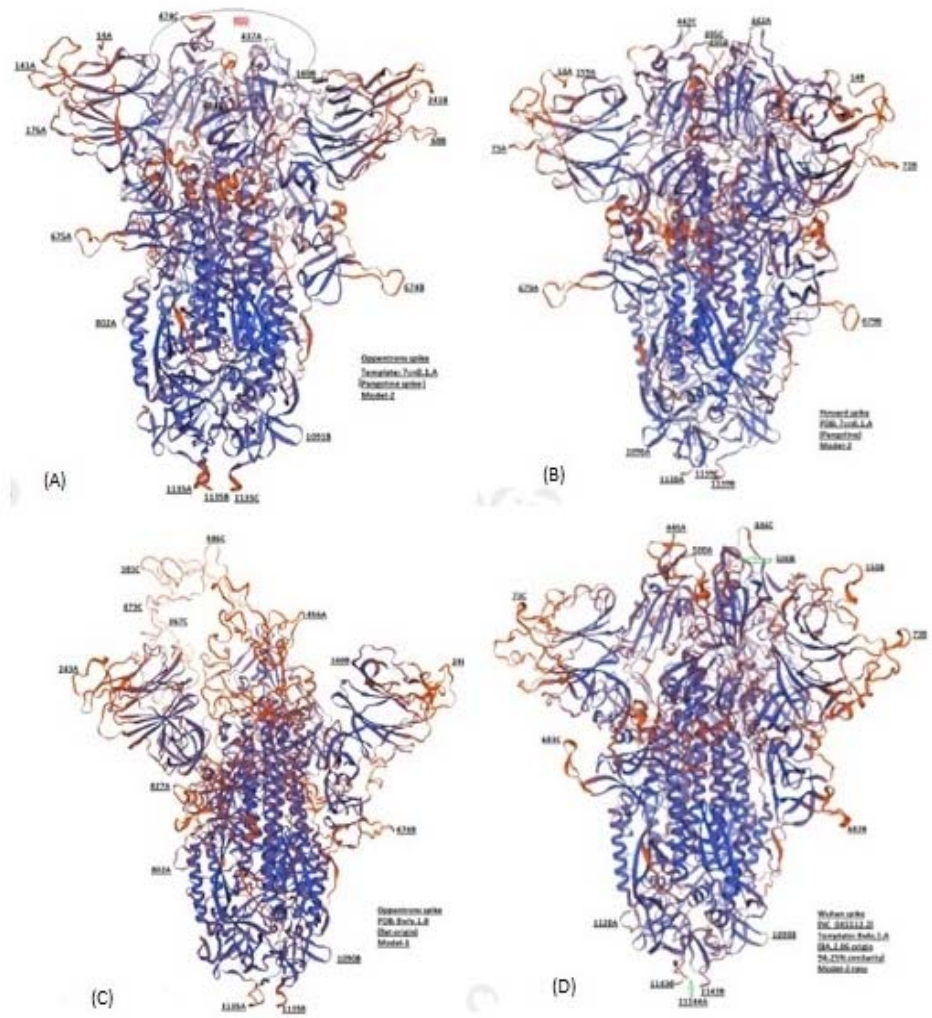

Figure 11: Swiss Modelling of spike with trimeric 3-D structures. (A) 3-D structures of the trimeric spike protein of JN.1 omicron coronaviruses by Oppentrons-spike with no 17MPLF spike insertion. (B). 3-D structure of trimeric spike protein with 17MPLF spike insertion or Howard-spike. (C) The Model structure of the Oppentrons-spike shows a trimeric spike with protruding subunit-C hindering interaction with ACE-2 receptors. (D). The model structure of the Wuhan spike originated in 2019.

Table 1: Omicron coronaviruses spike protein point mutations compared with Wuhan (protein id. YP_009724390). Variant B = Wuhan (2019-2020), Variant 1 = BA.1 (2021), Variant 2 = BA. 2 (2022), Variant 5 = BA.5 (2022) and Variant J = JN.1 (2024). POS = Amino acid position concerning Wuhan Spike. Similar changes between BA.2 and BA.2 are indicated by green color. Maroon colour means similar amino acid changes between BA.5 and JN.1.

Table-1A: Spike protein amino acid point mutations in Omicron BA.1 coronavirus (protein id. UKN08549)

POS	67	211	339	371	373	375	417	440	446	477	484	493	496	498	501	505	547	614	655	681	764	796	856	954	981				
B	A	N	G	S	S	S	K	N	G	S	E	Q	G	Q	N	Y	T	D	H	P	N	D	N	Q	L				
1	V	I	D	L	P	F	N	K	S	N	A	R	S	R	Y	H	K	G	Y	H	K	Y	K	H	F				

Table 1B: Spike protein amino acid point mutations in Omicron BA.2 coronavirus (protein id. UML40832)

POS	19	27	142	213	339	371	373	375	405	408	417	440	441	484	493	498	501	505	614	655	679	681	764	796	798	954	969		
B	T	A	G	V	G	S	S	S	D	R	K	N	T	E	Q	Q	N	Y	D	H	N	P	N	D	G	Q	N		
2	I	S	D	G	D	F	P	F	N	S	N	K	K	A	R	R	Y	H	G	Y	K	H	K	Y	N	H	K		

Table 1C: Spike protein amino acid point mutations in Omicron BA.5 coronaviruses (protein id. URO63244)

POS	3	19	27	142	213	339	371	373	375	376	405	408	417	440	452	477	478	484	486	498	501	505	614	655	679	796	954	969	
B	V	T	A	G	V	G	S	S	S	T	D	R	K	N	L	S	T	E	F	Q	N	Y	D	H	N	D	Q	N	
5	G	I	S	D	G	D	F	P	F	A	N	S	N	K	R	N	K	A	V	R	Y	H	G	Y	K	Y	H	K	

Table 1D: Spike protein amino acid point mutations in Omicron JN.1 coronavirus (protein id. WUY16791).

POS	19	21	27	50	127	142	157	158	177	212	213	216	245	264	332	339	356	371	373	375	376	403	405	408	417	440	445	446	450
B	T	R	A	S	V	G	F	R	M	L	V	L	H	A	I	G	K	S	S	S	T	R	D	R	K	N	V	G	N
J	I	T	S	L	F	D	S	G	I	I	G	F	N	D	V	H	T	F	P	F	A	K	N	S	N	K	H	S	D

POS	452	455	460	477	478	481	484	486	498	501	505	614	621	655	679	681	764	796	939	940	969	1143							
B	L	L	N	S	T	N	E	F	Q	N	Y	D	P	H	N	P	N	D	S	Q	N	P							
J	W	S	K	N	K	K	K	P	R	Y	H	G	S	Y	K	R	K	Y	F	H	K	L							

Table 2: Deletions and Insertions in the spike protein of different coronavirus variants.

Variant	Length (S)	Deletion in the Spike protein	Insertion in the Spike protein
Wuhan (B)	1273 AA	no	no
Alpha (B.1.1.7)	1270 AA	^{69}HV ^{145}Y	no
Beta (B.1.315)	1273 AA	^{241}LAL	no
Delta (B.1.617.2)	1271 AA	^{156}FR	no
Omicron BA.1	1270 AA	^{69}HV ^{143}VYY ^{212}L	^{215}EPE
Omicron BA.2	1270 AA	^{24}LPP	no
Omicron BA.4	1268 AA	^{24}LPP ^{69}HV	no
Omicron BA.5	1268 AA	^{24}LPP ^{69}HV	no
Omicron JN.1	1268 AA	^{24}LPP (^{31}S) ^{69}HV ^{145}Y ^{211}N ^{483}V	^{17}MPLF

Table 3: Parameters of SWISS-MODELLING of Spike Protein of SARS-CoV-2

Table 3A: Model-1: Parameters of Swiss-Modelling between spike protein of Howard and Oppentrons using template 8wly.1.B (Bat origin)

Author Protein id	QMQE	QSQE	Identity	MolProbity score	Clash score	Ramachandran favoured	Bad bonds	Bad angles
Howard XDF23570	0.69	0.99	74.64%	1.67	1.11	88.42%	1	214
Oppentrons XBS50626	0.68	0.98	77.00%	1.63	0.95	88.62%	0	201

Table 3B: Model-2: Parameters of Swiss-Modelling between spike protein of Oppentrons and Howard using template 7cn8.1.A (Pangolone origin)

Author Protein id	QMQE	QSQE	Identity	MolProbity score	Clash score	Ramachandran favoured	Bad bonds	Bad angles
Howard XDF23570	0.68	0.97	88.90%	1.45	0.90	94.90%	0	125
Oppentrons XBS50626	0.67	0.95	88.57%	1.38	0.63	93.87%	3	142

Table 3C: Model-3: Parameters of Swiss-Modelling between spike protein of Oppentrons and Howard using template 8xut.1.A (XBB.1.5.70 human origin)

Author Protein id	QMQE	QSQE	Identity	MolProbity score	Clash score	Ramachandran favoured	Bad bonds	Bad angles
Howard XDF23570	0.68	0.95	96.99%	1.80	0.95	87.65%	6	210
Oppentrons XBS50626	0.67	0.95	96.67%	1.76	0.89	85.00%	8	197

higher transmission with JN.1 coronaviruses although such variants were less pathogenic than alpha and delta variants that claimed six million deaths worldwide between 2020-2022. Previously, we reported a more colourful 3-D oligomeric spike in JN.1 coronavirus [20]. Keeping our argument short, we declared that +^{17}MPLF spike insertion was a favourable consequence in JN.1 coronaviruses [47].

In Table, we showed the parameters of Swiss modelling using the 8xut.1.A template. As the spike was XBB.1.5.70 variant and closer to JN.1 variant, we showed 96.99% similarity with JN.1 spike but only 87.65% Ramachandran favoured as well as MolProbity score was also increased to 1.80 whereas our best-fit model-2 gave only 1.45 MolProbity score. We expected a better symmetry in structure but our models failed so indicating Spike-ACE-2 interaction solely depends on the primary sequence of spike and mutations cause problems in virus assembly, transmission and optimum titre formation. Further, Swiss Modelling solely depends on template assignment to compare with and still, we could not understand why JN.1 spike of both Howard and Oppentrons failed to form a trimeric 3-D structure with increased MolProbity score to 1.9 and Clash score to 2.09 while the QSQE remained same (0.95) in case of 8gtp.1.B template having BA.5 human origin and 96.52% homology to JN.1 spike. It may be possible that the Cryo-EM procedures may not be the same and sensitivities may vary. The Model structure of the oppentrons spike showed a trimeric spike with protruding subunit-C hindering interaction into ACE-2 receptors as compared with 8wly.1.B template (Figure 11B). A similar but less protruding 3-D structure was obtained with the Howard spike and Wuhan spike (data not shown). Thus, Modelling of oligomeric proteins may be a good informatics showing protein structure and function. Surely, we introduced such data to explain the unsuitability of JN.1 spike without +^{17}MPLF four amino acid insertion as the spike already lost eight to nine amino acids (^{24}LPP, (^{31}S), ^{69}HV, ^{145}Y, ^{211}N and ^{483}V), The Wuhan spike gave trimeric structures in different templates but best one obtained with clash score 1.83 with 7cn8.1.A template gave a worse 3-D structure with 8wly.1 template with a clash score of 1.22 (data not shown). However, we must compare with the Wuhan spike and in Figure 11D we showed a 3-D model of the Wuhan spike (2019 coronavirus) using 8x4z.1.A template which was BA.2.86 variant origin and closer to the JN.1 variant. However, during our search using Swiss-Model such a template was not found with JN.1 spike either sequenced data by Oppentrons or Howard (Figure 11C).

Haseeb, et al. used in silico computational tools to analyse the SARS-CoV-2 spike proteins of different variants using the Swiss Model. The Clash score of B.1.1.7 spike was found 0.82 which was changed to 1.35 in the delta spike although

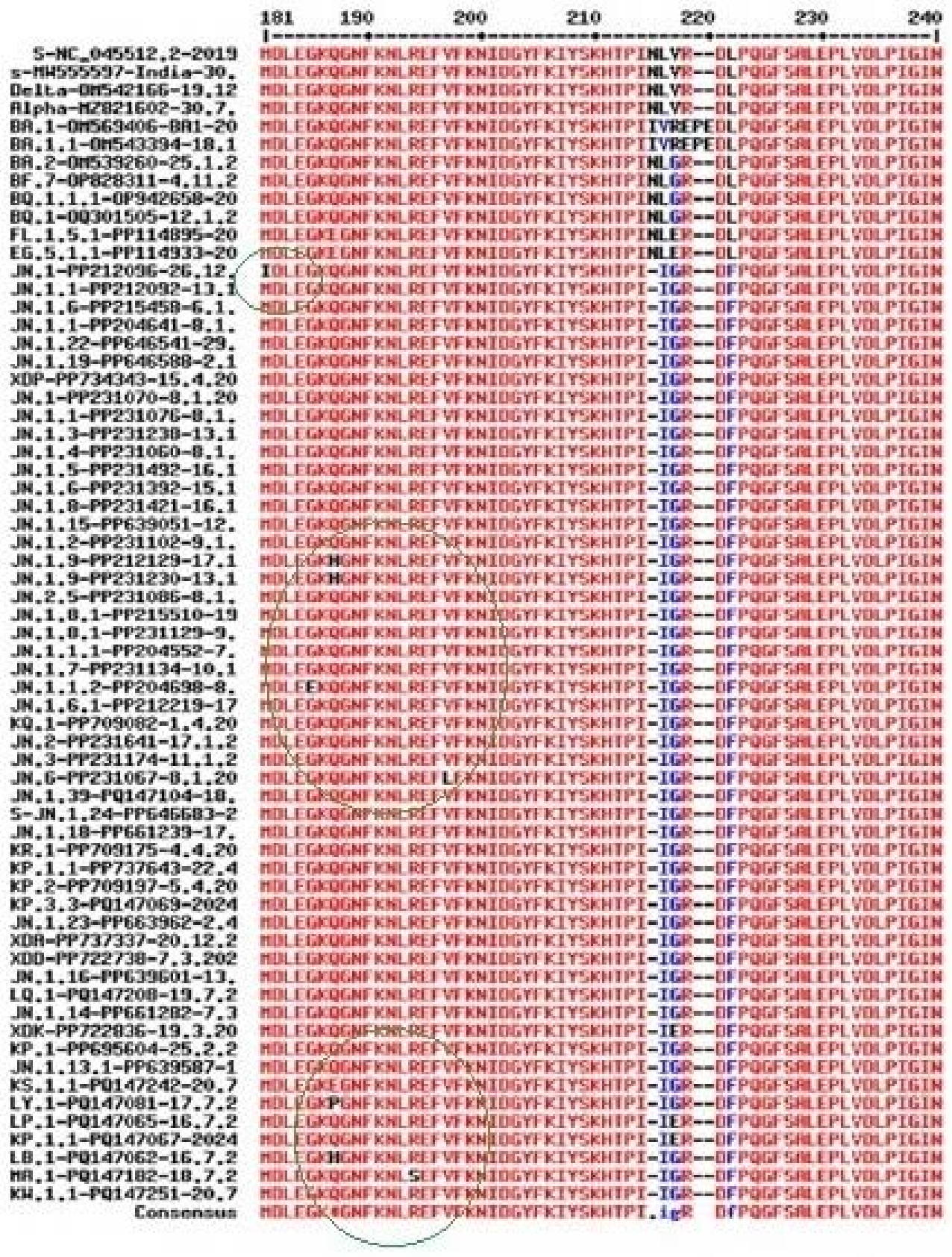

Figure 12: Spike multi-alignment of JN.1 lineages to demonstrate the cluster of mutations (black letters) that occurred upstream of the RBD domain (181-200aa positions) and rarely found at the carboxy terminus of the spike. The EPE insertion in omicron BA.1 only and ^{211}N deletion in JN.1 lineages only are also shown. Part of the alignment was reported due to the page limit. Thus, the deletions, insertions and point mutations all allowed in the spike of JN.1 lineages at the NH_2-terminus to make a compact 3-D trimeric spike to bind the ACE-2 receptor.

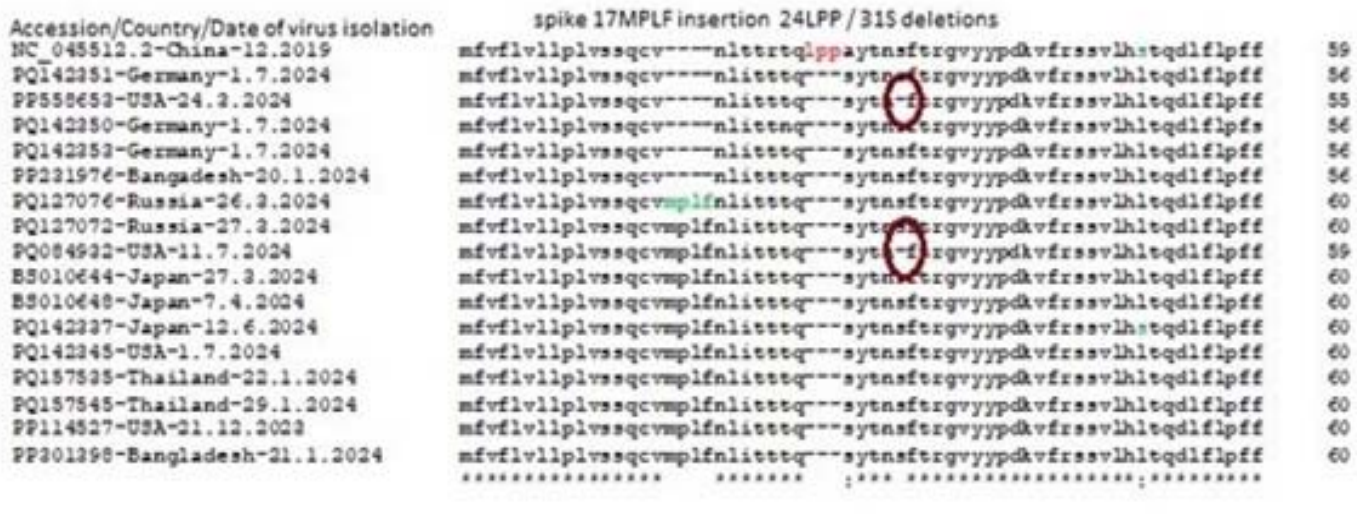

Figure 13: Demonstration of controversial [17]MPLF spike insertion in JN.1 omicron coronaviruses from different countries. Even the same country but different researchers had opposite results which must be resolved.

MolProbity was found very same (1.56 *vs.* 1.55) whereas the Clash score for Wuhan 3.19 was high as also reflected in our analysis [48]. Ortega, et al. demonstrated using silica analysis that Omicron SARS-CoV-2 Variant Spike Protein had an increased affinity to the human ACE-2 Receptor [49]. The delta variant with L452R and T478K mutations in RBD did not interact directly with the ACE-2 receptor but immune evasion properties were demonstrated. However, R493, S496, R498, Y501 and H505 mutations in the omicron interacted directly with the ACE-2.

Next, we demonstrated the LB.1 variant L5F, A168V & Q180H, LY.1 variant F60S & Q181, KS.1.1 variant T26N & Q181E, KP.3.3 variant Q512E, KW.1.1 variant Q511E and MA.1 variant L469V mutations were found (Figure 12). But no spike amino acid changes at the RBD domain demonstrated such subvariants were very similar to JN.1 lineages. Similarly, we aligned a few COVID-19 JN.1 sequences from different countries to demonstrate that different researchers in the same country had opposite views as shown in Figure 13. Surely, such spike sequence controversy must be resolved (Research Square, 15th July, 2024).

Surely, JN.1 specific vaccine development is needed because of continuous changes in the spike due to the pressure of monoclonal spike immune drugs and spike vaccines. However, important drugs targeting protease (Nirmatrelvir, Leritrelvir) and RNA-dependent RNA Polymerase (Remdesivir, Favipiravir) will be at the centre stage of COVID-19 therapy. Truly, immune drugs (Bamlanivimab, Etesvimab) are very costly for the poor people of India but still are used in a few cases to treat rich patients [50,51]. Thus, due to continuous changes in the different coronavirus variants, repeated coronavirus infections will be seen worldwide and we should never fabricate coronavirus sequencing data [52].

Conclusion

We concluded that pre-elimination of COVID-19 was initiated with more and more deletions in the 3'-UTR as well as the NH_2-terminus of the spike. At least part of the deletions were compensated through the [17]MPLF four amino acids spike insertion. The 49nt 3'-UTR deletion was continuing making coronaviruses more fragile with low titre. The Oppentrons and Atkins spike without [17]MPLF insertion reflected an error during RNA sequencing! The Swiss modelling demonstrated that the JN.1 variant with nine AAs deletions and four AAs insertions of spike formed a more stable 3-D structure reflecting higher transmission. We claim that Howard, et al. are doing excellent work on coronavirus whole genome sequencing.

Acknowledgement

We thank free CLUSTAL-Omega software and free SARS-CoV-2 database availability from NIH, USA. The article was deposited to Research Square Preprint (21st August 2024).

Ethical issues

This is computer-generated data and no animal or human is directly used in this study.

References

1. Lu R, Zhao X, Li J, Niu P, Yang B, Wang W, et al. Genomic characterisation and epidemiology of 2019 novel coronavirus: Implications for virus origins and receptor binding. Lancet. 2020;395:565-574. Available from: https://www.thelancet.com/journals/lancet/article/PIIS0140-6736(20)30251-8/fulltext

2. Peiris M, Poon LLM. Severe Acute Respiratory Syndrome (SARS) and Middle East Respiratory Syndrome (MERS) (Coronaviridae). In: Encyclopedia of Virology. 2021;814–824. Available from: https://doi.org/10.1016%2FB978-0-12-814515-9.00138-7

3. Chakraborty AK. Conversion of B.0 lineage of human coronavirus (Covid-19) into notoriously infecting less pathogenic and immune

escape omicron B.1.1.529.2.75.2 or BA.2.75.2 variant. J Biomed Res Reports. 2023;2(10). Available from: https://crimsonpublishers.com/cjmi/pdf/CJMI.000648.pdf

4. Lu G, Wang Q, Gao GF. Bat-to-human: spike features determining 'host jump' of coronaviruses SARS-CoV, MERS-CoV, and beyond. Trends Microbiol. 2015;23:468-478. Available from: https://doi.org/10.1016/j.tim.2015.06.003

5. Chakraborty AK, Chanda A. New Biotechnological Exploration on COVID-19 Proteins: Functions, Mutational Profiles and Molecular Targets for Drug Design. Sun Text Rev Virol. 2021;2(1):115. Available from: http://dx.doi.org/10.51737/2766-5003.2021.015

6. Das S, Kar SS, Samanta S, J. Banerjee, Giri B, Dash SK, et al. Immunogenic and reactogenic efficacy of Covaxin and Covishield: a comparative review. Immunol Rs. 2022;70(3):289-315. Available from: https://doi.org/10.1007%2Fs12026-022-09265-0

7. Jackson CB, Farzan M, Chen B, Choe H. Mechanisms of SARS-CoV-2 entry into cells. Nat Rev Mol Cell Biol. 2022;23(1):3-20. Available from: https://doi.org/10.1038/s41580-021-00418-x

8. Huang N, Pérez P, Kato T, Mikami Y, Okuda K. SARS-CoV-2 infection of the oral cavity and saliva. Nat Med. 2021;27(5):892-903. Available from: https://doi.org/10.1038/s41591-021-01296-8

9. Chakraborty AK. Hyper-variable Spike Protein of Omicron Corona Virus and its differences with Alpha and Delta Variants: Prospects of RT-PCR and new Vaccine. J Emerg Dis Virol. 2022;7(1):1-13. Available from: https://www.sciforschenonline.org/journals/virology/article-data/JEDV166/JEDV166.pdf

10. Korber B, Fischer WM, Gnanakaran S, Yoon H, Theiler J, Montefiori DC, et al. Tracking changes in SARS-CoV-2 spike: Evidence that D614G increases infectivity of the COVID-19 virus. Cell. 2020;182:812-827. Available from: https://doi.org/10.1016/j.cell.2020.06.043

11. Liu Y, Liu J, Plante KS, Plante JA, Xie X, Zhang X, et al. The N501Y spike substitution enhances SARS-CoV-2 infection and transmission. Nature. 2022;602(7896):294-299. Available from: https://doi.org/10.1038/s41586-021-04245-0

12. Gobeil S, Janowska K, McDowell S, Mansouri K, Parks R, Stalls V, et al. Effect of natural mutations of SARS-CoV-2 on spike structure, conformation, and antigenicity. Science. 2021;373(6555). Available from: https://doi.org/10.1126/science.abi6226

13. Chakraborty AK. Coronavirus Nsp2 Protein Homologies to the Bacterial DNA Topoisomerase I and IV Suggest Nsp2 Protein is a Unique RNA Topoisomerase with Novel Target for Drug and Vaccine Development. Virol Mycol. 2020;9:185. Available from: https://www.longdom.org/open-access/coronavirus-nsp2-protein-homologies-to-the-bacterial-dna-topoisomerase-i-and-iv-suggest-nsp2-protein-is-an-unique-rna-topoisomeras-53774.html

14. Han P, Li L, Liu S, Fu L, Gao GF, Wang P. Receptor binding and complex structures of human ACE2 to spike RBD from omicron and delta SARS-CoV-2. Cell. 2022;185(4):630-640.e10. Available from: https://doi.org/10.1016/j.cell.2022.01.001

15. Sheward DJ, Kim C, Fischbach J, Sato K, Muschiol S, Ehling RA, et al. Omicron sub-lineage BA.2.75.2 exhibits extensive escape from neutralising antibodies. Lancet Infect Dis. 2022;22(11):1538-1540. Available from: https://doi.org/10.1016/s1473-3099(22)00663-6

16. Wang Q, Iketani S, Li Z, Liu L, Guo Y, Huang Y, et al. Alarming antibody evasion properties of rising SARS-CoV-2 BQ and XBB subvariants. Cell. 2023;186(2):279-286.e8. Available from: https://doi.org/10.1016/j.cell.2022.12.018

17. Zhang J, Xiao T, Cai Y, Chen B. Structure of SARS-CoV-2 spike protein. Curr Opin Virol. 2021;50:173-182. Available from: https://doi.org/10.1016%2Fj.coviro.2021.08.010

18. Wang Q, Guo Y, Liu L, Schwanz LT, Li Z, Nair MS, Ho J, et al. Antigenicity and receptor affinity of SARS-CoV-2 BA.2.86 spike. Nature. 2023;624 (7992):639-644. Available from: https://doi.org/10.1038/s41586-023-06750-w

19. Chakraborty AK. The 249RWMD spike protein insertion in Omicron BQ.1 subvariant compensates the 24LPP and 69HV deletions and may cause more severe disease than BF.7 and XBB.1 subvariants. Int J Clin Med Edu Res. 2023;2(10):254-270. Available from: https://www.opastpublishers.com/open-access-articles/the-249rwmd-spike-protein-insertion-in-omicron-bq1-subvariant-compensates-the-24lpp-and-69hv-deletions-and-may-cause-sev.pdf

20. Chakraborty AK. Higher omicron JN.1 and BA.2.86.1 coronavirus transmission due to unique 17MPLF spike insertion compensating 24LPP, 69HV, 145Y, 211N and 483V deletions in the spike. J Future Med Healthcare Innovation. 2024;21(1):1-20. Available from: https://www.opastpublishers.com/open-access-articles/higher-omicron-jn1-and-ba2861-coronavirus-transmission-due-to-unique17-mplf-spike-insertion-compensating-24lpp-69hv-145y.pdf

21. Gao Y, Yan L, Huang Y, Liu F, Zhao Y, Cao L, et al. Structure of the RNA-dependent RNA polymerase from COVID-19 virus. Science. 2020;368: 779-782. Available from: https://doi.org/10.1126/science.abb7498

22. Chakraborty AK. Dynamics of SARS-CoV-2 ORF7a Gene Deletions and Fate of Downstream ORF7b and ORF8 Genes Expression. SunText Rev Biotechnol. 2022;3(1):142. Available from: https://doi.org/10.51737/2766-5097.2022.042

23. Chakraborty AK. Highly Infectious, Less Pathogenic and Antibody Resistant Omicron Xbb.1, Xbb.1.5 and Xbb.1.5.1- Xbb.1.5.39 Subvariant Coronaviruses Do Not Produce Orf8 Protein Due To 8th Codon Gga=Tga Termination Codon Mutation. Cohesive J Microbiol Infect Dis. 2023;6(5).000648. Available from: https://crimsonpublishers.com/cjmi/pdf/CJMI.000648.pdf

24. Chakraborty AK. SARS-CoV-2 ORF8 gene CAA=TAA and AAA=TAA termination codon mutations found mostly in B.1.1.7 variant was independent of popular L84S mutations. Int J Clin Med Edu Res. 2022;1(6):192-208. Available from: https://www.opastpublishers.com/open-access-articles/sarscov2-orf8-gene-caataa-and-aaataa-termination-codon-mutations-found-mostly-in-b117-variants-was-independent-of-popula.pdf

25. Chakraborty AK. Rapid worldwide spread of 17MPLF spike insertion mutants (JN.1-JN.1.25, KP.1, KP.2, KQ.1, KR.1, XDD, XDP, XDK, XDQ subvariants) of omicron coronaviruses and spike gene 5'-end sequencing problem. Res Square. 2024. Available from: https://doi.org/10.21203/rs.3.rs-4741070/v1

26. Yang Y, Jiang XT, Zhang T. Evaluation of a Hybrid Approach using UBLAST and BLASTX for Metagenomic Sequences Annotation of specific functional genes. PLoS One. 2014;9(10). Available from: https://doi.org/10.1371%2Fjournal.pone.0110947

27. Altschul SF, Gish W, Miller W, Myers EW, Lipman DJ. Basic local alignment search tool. J Mol Biol. 1990;215:403–410. Available from: https://doi.org/10.1016/s0022-2836(05)80360-2

28. Corpet F. Multiple sequence alignment with hierarchical clustering. Nucleic Acids Res. 1988;16:10881-10890. Available from: https://doi.org/10.1093%2Fnar%2F16.22.10881

29. Wallace IM, Blackshields G, Higgins DG. Multiple sequence alignments. Curr Opin Struct Biol. 2005;15(3):261–266. Available from: https://doi.org/10.1016/j.sbi.2005.04.002

30. Sievers F, Wilm A, Dineen DG, Gibson TJ, Karplus K, Li W, et al. Fast, scalable generation of high-quality protein multiple sequence alignments using Clustal Omega. Mol Syst Biol. 2011;7:539. Available from: https://doi.org/10.1038/msb.2011.75

31. Waterhouse A, Bertoni M, Bienert S, Studer G, Tauriello G, Gumienny R, et al. SWISS-MODEL: homology modelling of protein structures and complexes. Nucleic Acids Res. 2018;46. Available from: https://doi.org/10.1093%2Fnar%2Fgky427

32. Studer G, Tauriello G, Bienert S, Biasini M, Johner N, Schwede T. A versatile homology modelling toolbox. PLoS Comput Biol. 2021;17(1). Available from: https://doi.org/10.1371/journal.pcbi.1008667

33. Varadi M, Anyango S, Deshpande M, Nair S, Natassia C, Yordanova G, et al. AlphaFold protein structure database: massively expanding the structural coverage of protein-sequence space with high accuracy models. Nucleic Acids Res. 2022;50. Available from: https://doi.org/10.1093/nar/gkab1061

34. Zhao J, Qiu J, Aryal S, Hackett JL, Wang J. The RNA Architecture of the SARS-CoV-2 3'-Untranslated Region. Viruses. 2020;12(12):1473. Available from: https://doi.org/10.3390/v12121473

35. Hendrickson EN, Ericson ME, Bemis LT. Host tRNA-Derived RNAs Target the 3'-Untranslated Region of SARS-CoV-2. Pathogens. 2022;11(12): 1479. Available from: https://doi.org/10.3390/pathogens11121479

36. Hernández-Huerta MT, Pérez-Campos Mayoral L, Matias-Cervantes CA, Romero Díaz C, Cruz Parada E, Pérez-Campos Mayoral E, et al. 3'-UTR of the SARS-CoV-2 genome as a possible source of piRNAs. Genes Dis. 2023;10(3):668-670. Available from: https://doi.org/10.1016/j.gendis.2022.05.028

37. Pérez-Campos Mayoral L, Hernández-Huerta MT, Romero Díaz C, Matias-Cervantes CA, Pérez-Campos Mayoral E, Martínez Cruz M, et al. Interaction of piRNA-like sequences from the 3'-UTR of SARS-CoV-2 with mRNA regions. Genes Dis. 2023;10(6):2282-4. Available from: https://doi.org/10.1016%2Fj.gendis.2023.01.012

38. Mukherjee M, Goswami S. Global cataloguing of variations in untranslated regions of viral genome and prediction of key host RNA binding protein-microRNA interactions modulating genome stability in SARS-CoV-2. PLoS One. 2020;15(8). Available from: https://doi.org/10.1371%2Fjournal.pone.0237559

39. Meseguer S, Rubio MP, Lainez B, Pérez-Benavente B, Pérez-Moraga R, Romera-Giner S, et al. SARS-CoV-2-encoded small RNAs are able to repress the host expression of SERINC5 to facilitate viral replication. Front Microbiol. 2023;14:1066493. Available from: https://doi.org/10.3389/fmicb.2023.1066493

40. Hagey RJ, Elazar M, Pham EA, Tian S, Ben-Avi L, Bernardin-Souibgui C, et al. Programmable antivirals targeting critical conserved viral RNA secondary structures from influenza A virus and SARS-CoV-2. Nat Med. 2022;28(9):1944-1955. Available from: https://doi.org/10.1038/s41591-022-01908-x

41. Chakraborty AK. Multi-Alignment Comparison of Coronavirus Non-Structural Proteins Nsp13-16 with Ribosomal Proteins and Other DNA/RNA Modifying Enzymes Suggested Their Roles in the Regulation of Host Protein Synthesis. Int J Clin Med Informatics. 2020;3:7-19. Available from: https://osf.io/preprints/indiarxiv/qrxc5

42. Zhang J, Cai Y, Lavine CL, Lu J, Xiao T, Chen B. Structural and functional impact by SARS-CoV-2 Omicron spike mutations. Cell Rep. 2022;39(4):110729. Available from: https://doi.org/10.1016/j.celrep.2022.110729

43. McCallum M, Walls AC, Bowen JE, et al. Structure-guided covalent stabilization of coronavirus spike glycoprotein trimers in the closed conformation. Nat Struct Mol Biol. 2020;27:942-949. Available from: https://doi.org/10.1038/s41594-020-0483-8

44. Ou X, Guan H, Qin B, Corti D, Veesler D. Crystal structure of the receptor binding domain of the spike glycoprotein of human betacoronavirus HKU1. Nat Commun. 2017;8:15216. Available from: https://www.nature.com/articles/ncomms15216

45. Walls AC, Tortorici MA, Bosch BJ, Frenz B, Rottier PJM, DiMaio F, et al. Cryo-electron microscopy structure of a coronavirus spike glycoprotein trimer. Nature. 2016;531(7592):114-117. Available from: https://doi.org/10.1038/nature16988

46. Dey S, Chakraborty P, Janin J. A survey of haemoglobin quaternary structures. Proteins. 2011;79(10):2861-2870. doi: 10.1002/prot.23112. Available from: https://doi.org/10.1002/prot.23112

47. Lemmin T, Kalbermatter D, Harder D, Plattet P, Fotiadis D. Structures and dynamics of the novel S1/S2 protease cleavage site loop of the SARS-CoV-2 spike glycoprotein. J Struct Biol. 2020;4:100038. doi: 10.1016/j.yjsbx.2020.100038. Available from: https://doi.org/10.1016/j.yjsbx.2020.100038

48. Haseeb M, Amir A, Ikram A. In Silico Analysis of SARS-CoV-2 Spike Proteins of Different Field Variants. Vaccines (Basel). 2023 Mar 27; 11(4):736. Available from: https://doi.org/10.3390%2Fvaccines11040736

49. Ortega JT, Jastrzebska B, Rangel HR. Omicron SARS-CoV-2 Variant Spike Protein shows an increased affinity to the Human ACE2 Receptor: An in-silico analysis. Pathogens. 2021;11(1):45. Available from: https://doi.org/10.3390/pathogens11010045

50. Choi HS, Choi AY, Kopp JB, Winkler CA, Cho SK. Review of COVID-19 therapeutics by mechanism: from discovery to approval. J Korean Med Sci. 2024;39(14). Available from: https://doi.org/10.3346/jkms.2024.39.e134

51. Wang H, Xue Q, Zhang H, Yuan G, Wang X, Sheng K, et al. Neutralization against omicron subvariants after BA.5/BF.7 breakthrough infection weakened as virus evolution and ageing despite prototype-based vaccination. Emerg Microbes Infect. 2023;12(2):2249121. Available from: https://doi.org/10.1080/22221751.2023.2249121

52. Yang S, et al. Fast evolution of SARS-CoV-2 BA.2.86 to JN.1 under heavy immune pressure. Lancet Infect Dis. 2023;15(23).